

# Electronic Supplementary Information

## Nanostructured terbium-doped ceria spheres: Effect of dopant on physical and chemical properties under reducing and oxidizing conditions

*Leandro M. Acuña<sup>1,2</sup>, Fernando F. Muñoz<sup>1,2</sup>, Cecilia A. Albornoz<sup>3</sup>, A. Gabriela*

*Leyva<sup>3,4</sup>, Richard T. Baker<sup>5</sup> and Rodolfo O. Fuentes<sup>\*,2,3</sup>*

<sup>1</sup> CINSO (Centro de Investigaciones en Sólidos), CONICET-CITEDEF, J.B. de La Salle 4397, 1603 Villa Martelli, Buenos Aires, Argentina.

<sup>2</sup> CONICET, Buenos Aires, Argentina.

<sup>3</sup> Departamento de Física, Centro Atómico Constituyentes, CNEA, Av. Gral. Paz 1499, (1650) San Martín, Buenos Aires, Argentina.

<sup>4</sup> Escuela de Ciencia y Tecnología, Universidad Nacional de San Martín, M. de Yrigoyen 3100, (1650) San Martín, Buenos Aires, Argentina.

<sup>5</sup> EaStChem, School of Chemistry, University of St. Andrews, North Haugh, St. Andrews, Fife, KY16 9ST, United Kingdom.

\* Corresponding author: rofuentes@conicet.gov.ar.

**Table 1.** Structural parameters and standard Rietveld agreement factor for nanostructured TbDC10 spheres (HMW).

Atmosphere	Air	5%H <sub>2</sub> /He	5%H <sub>2</sub> /He	21%O <sub>2</sub> / N <sub>2</sub>	21%O <sub>2</sub> / N <sub>2</sub>
<i>T</i> (°C)	25	300	500	500	25
<i>a</i> (Å)	5.4069(6)	5.4223(9)	5.4472(8)	5.4347(8)	5.4038(8)
<i>V</i> (Å <sup>3</sup> )	158.077(3)	159.422(5)	161.629(4)	160.525(4)	157.798(4)
<i>R<sub>p</sub></i>	3.22	3.55	3.64	3.64	3.20
<i>R<sub>wp</sub></i>	3.84	4.24	4.33	4.29	3.93
<i>R<sub>e</sub></i>	2.29	2.25	2.33	2.33	2.22
$\chi^2$	2.80	3.53	3.46	3.40	3.14

**Table 2.** Structural parameters and standard Rietveld agreement factor for nanostructured TbDC20 spheres (HMW).

Atmosphere	Air	5%H <sub>2</sub> /He	5%H <sub>2</sub> /He	21%O <sub>2</sub> / N <sub>2</sub>	21%O <sub>2</sub> / N <sub>2</sub>
<i>T</i> (°C)	25	300	500	500	25
<i>a</i> (Å)	5.4049(6)	5.4213(9)	5.4479(8)	5.4291(8)	5.3992(8)
<i>V</i> (Å <sup>3</sup> )	157.896(3)	159.337(5)	161.699(4)	160.025(4)	157.399(4)
<i>R<sub>p</sub></i>	3.06	3.04	3.59	3.35	3.34
<i>R<sub>wp</sub></i>	3.73	3.68	4.19	4.07	4.06
<i>R<sub>e</sub></i>	2.45	2.33	2.40	2.43	2.46
$\chi^2$	2.32	2.50	3.04	2.80	2.72

**Table 3.** Structural parameters and standard Rietveld agreement factor for nanostructured TbDC10 powder (CC).

Atmosphere	Air	5%H <sub>2</sub> /He	5%H <sub>2</sub> /He	21%O <sub>2</sub> / N <sub>2</sub>	21%O <sub>2</sub> / N <sub>2</sub>
<i>T</i> (°C)	25	300	500	500	25
<i>a</i> (Å)	5.4032(6)	5.4261(9)	5.4474(8)	5.4346(8)	5.4036(8)
<i>V</i> (Å <sup>3</sup> )	157.750(3)	159.761(5)	161.647(4)	160.511(4)	157.780(4)
<i>R<sub>p</sub></i>	2.39	2.90	3.37	3.16	2.50
<i>R<sub>wp</sub></i>	2.95	3.45	3.89	3.70	3.08
<i>R<sub>e</sub></i>	2.25	2.24	2.29	2.32	2.27
<i>χ<sup>2</sup></i>	1.72	2.39	2.89	2.55	1.84

**Table 4.** Structural parameters and standard Rietveld agreement factor for nanostructured TbDC20 powder (CC).

Atmosphere	Air	5%H <sub>2</sub> /He	5%H <sub>2</sub> /He	21%O <sub>2</sub> / N <sub>2</sub>	21%O <sub>2</sub> / N <sub>2</sub>
<i>T</i> (°C)	25	300	500	500	25
<i>a</i> (Å)	5.3931(6)	5.4118(9)	5.4484(8)	5.4219(8)	5.3891(8)
<i>V</i> (Å <sup>3</sup> )	156.862(3)	158.499(5)	161.736(4)	159.388(4)	156.516(4)
<i>R<sub>p</sub></i>	2.49	2.61	3.14	3.00	2.48
<i>R<sub>wp</sub></i>	3.06	3.28	3.79	3.68	3.21
<i>R<sub>e</sub></i>	2.44	2.33	2.44	2.48	2.47
<i>χ<sup>2</sup></i>	1.57	1.98	2.40	2.20	1.39

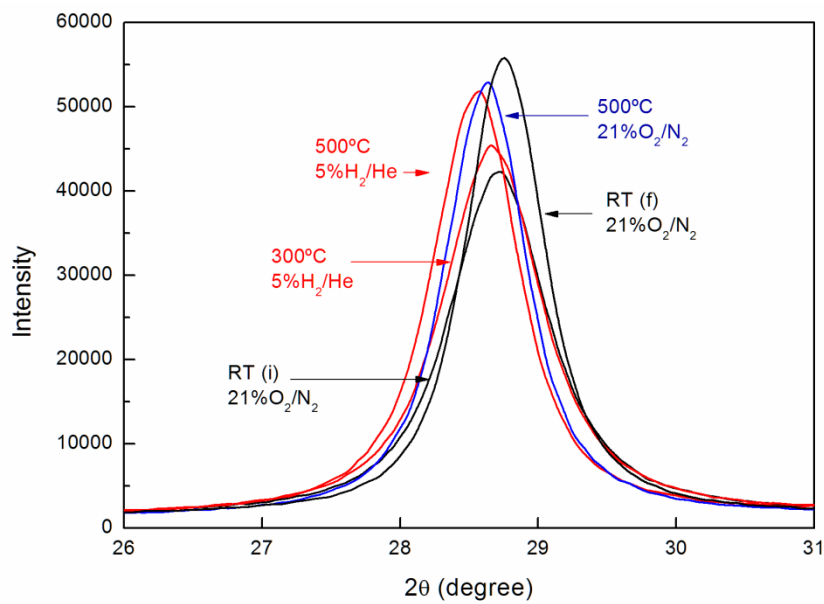


**Figure S1.** SR-XRD patterns in the vicinity of the 111 reflection for nanostructured TbDC10 spheres (HMW). RT (i) and (f) indicate the initial state (fresh sample) and final state (after exposure to the different redox conditions described in the text) of the sample, respectively.

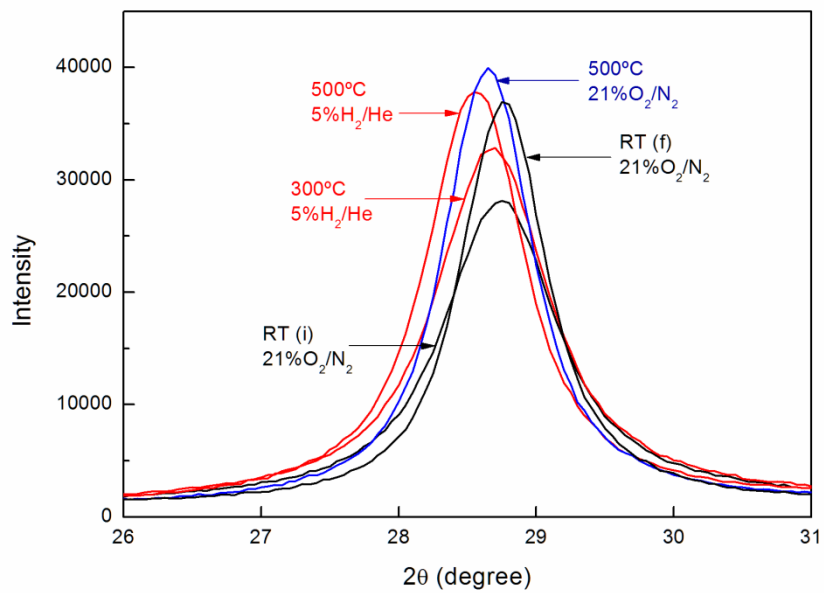


**Figure S2.** SR-XRD pattern in the vicinity of the 111 reflection for nanostructured TbDC20 spheres (HMW). RT (i) and (f) indicate the initial state (fresh sample) and final state (after exposure to the different redox conditions described in the text) of the sample, respectively.

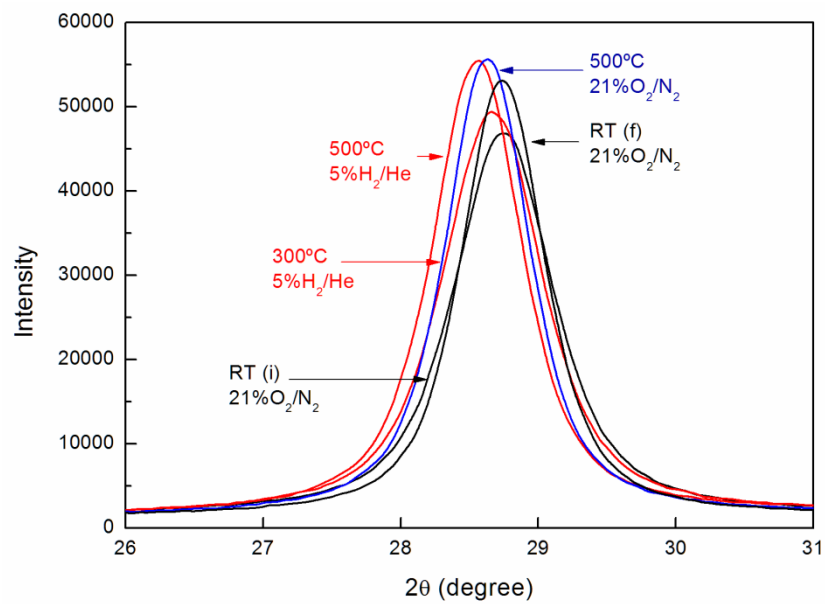


**Figure S3.** SR-XRD pattern in the vicinity of the 111 reflection for nanostructured TbDC10 powders (CC). RT (i) and (f) indicate the initial state (fresh sample) and final state (after exposure to the different redox conditions described in the text) of the sample, respectively.

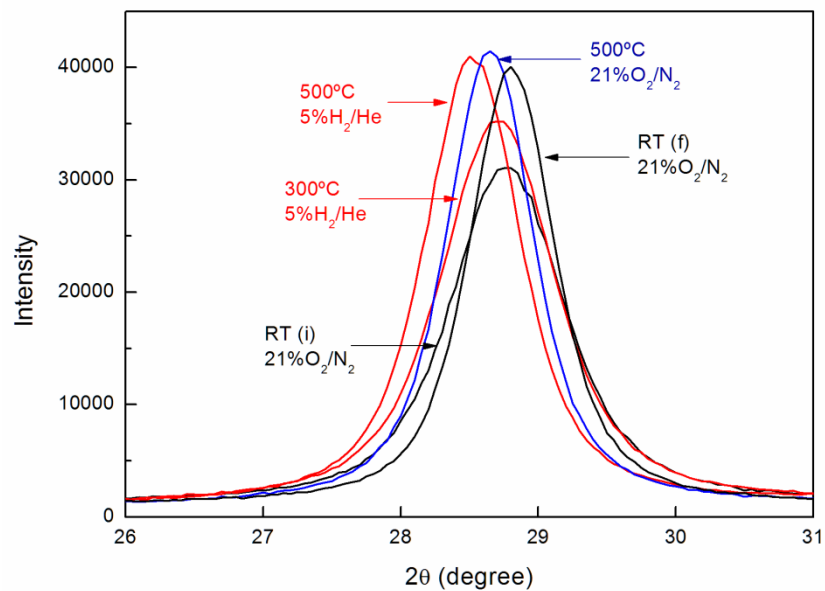


**Figure S4.** SR-XRD pattern in the vicinity of the 111 reflection for nanostructured TbDC20 powders (CC). RT (i) and (f) indicate the initial state (fresh sample) and final state (after exposure to the different redox conditions described in the text) of the sample, respectively.

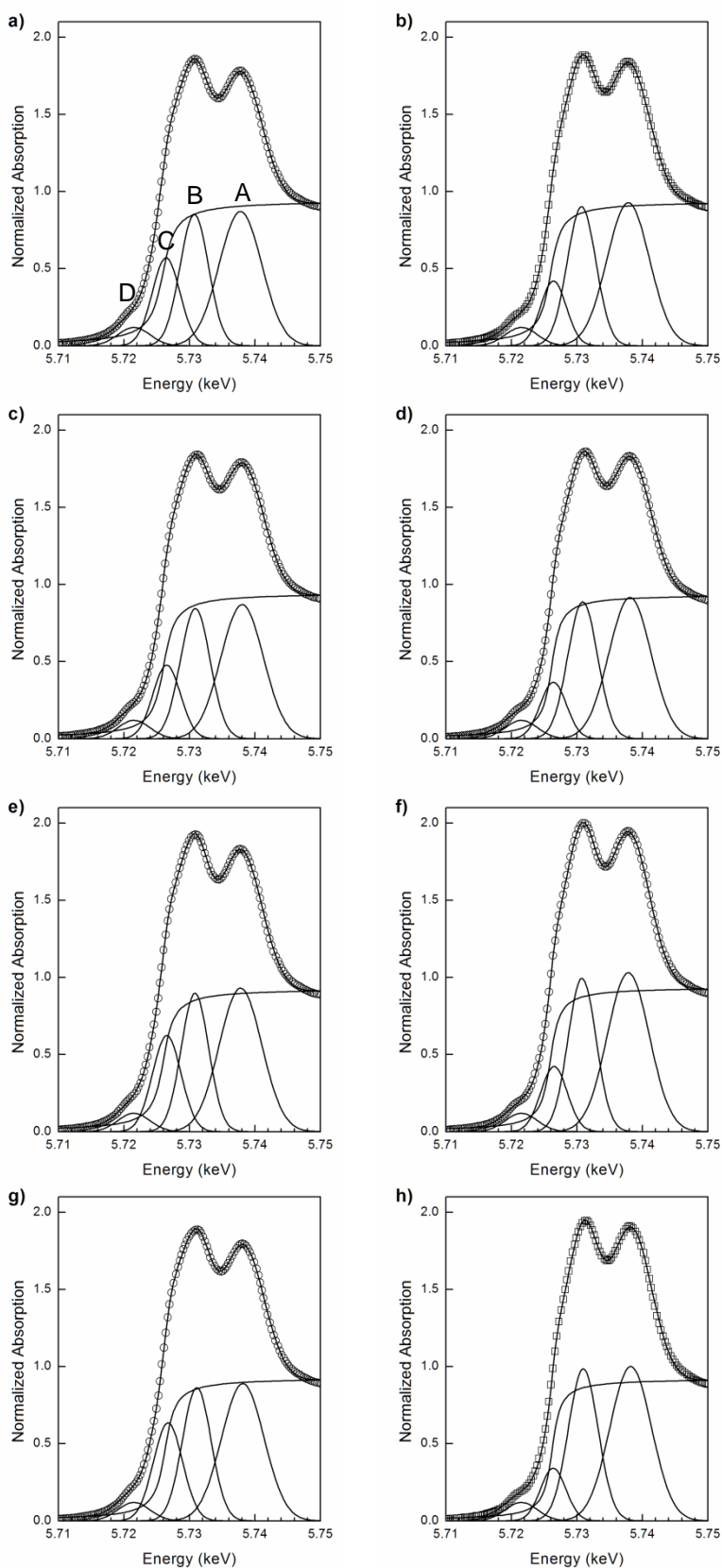


**Figure S5.** Normalized XANES spectra at the Ce L<sub>3</sub>-edge for TbDC10-HMW, TbDC20-HMW, TbDC10-CC and TbDC20-CC at 500 °C under (a, c, e and g) reducing and (b, d, f and h) oxidizing conditions, respectively, showing the experimental data (empty circles), four Gaussian peaks (A–D), one arctangent function obtained by least-squares fitting and the sum of all five functions (continuous line).